Quantum Control of Hole Spin Qubits in Double Quantum Dots

D. Fernández-Fernández[1], Yue Ban[2,3,4] and G. Platero[1,*]

[1]*Instituto de Ciencia de Materiales de Madrid ICMM-CSIC, Madrid 28049, Spain*
[2]*Department of Physical Chemistry, University of the Basque Country UPV/EHU, Bilbao, Spain*
[3]*EHU Quantum Center, University of the Basque Country UPV/EHU, Leioa, Biscay, Spain*
[4]*TECNALIA, Basque Research and Technology Alliance (BRTA), Derio, Bizkaia 48160, Spain*

Hole spin qubits in semiconductor quantum dots (QDs) are promising candidates for quantum information processing due to their weak hyperfine coupling to nuclear spins, and to the strong spin-orbit coupling, which allows for rapid operation time. We propose a coherent control on two heavy-hole spin qubits in a double QD by a fast adiabatic driving protocol, which helps to achieve higher fidelities than other experimentally commonly used protocols as linear ramping, π pulses or Landau-Zener passages. Using fast quasiadiabatic driving via spin-orbit coupling, it is possible to reduce charge noise significantly for qubit manipulation and achieve high robustness for the qubit initialization. We also implement one- and two-qubit gates, in particular, NOT, CNOT, and SWAPlike gates, of hole spins in a double QD achieving fidelities above 99%, exhibiting the capability of hole spins to implement universal gates for quantum computing.

I. INTRODUCTION

Fast and precise control of a large number of qubits is required for the implementation of quantum algorithms and hardware to realize quantum computing. As one of the pillars in the development of quantum technologies [1–5], spin qubits in quantum dots (QDs) [6–8] present long coherence time [9] and compatibility in semiconductor manufacturing technology [10]. Recent progress with a fidelity exceeding 99% overcomes the barrier for two-qubit gate control [11–14], which signifies that semiconductor qubits possess promising potential applications in the era of noisy intermediate-scale quantum devices. Great effort is currently being devoted to the investigation of hole spin qubits in QDs [15–30], owing to their long coherence time resulting from the weak hyperfine coupling to nuclear spins [18], and rapid operation time [20,31,32] due to the inherently strong spin-orbit coupling (SOC). In particular, Ge QDs [33–36] have high hole mobility and a strong Rashba SOC [31,37], which facilitates electrical drive for fast qubit operations. In GaAs QDs however, due to the lack of bulk inversion symmetry, Dresselhaus SOC also plays a role. All of these allow for a wide range of tunable properties, leading to highly scalable, easily addressable, and fast hole spin qubits. However, all-electric control related to strong SOC could induce a higher susceptibility to charge noise, which is detrimental to the robustness of hole spin qubits.

Landau-Zener (LZ) protocols have been developed to manipulate charge and spin electron qubits [38–42]. Low ramping velocity and adiabatic pulses allow for the transition along the instantaneous eigenstate [43,44], but are prone to decoherence, whereas fast ramping causes transitions between instantaneous eigenstates. Pulses in different shapes like "double hat," "convolved," and "trapezoid" [45] solve this trade-off to some extent. However, high accuracy needs further tuning of the parameters whose modulation can allow for the best compromise. To this end, shortcuts to adiabaticity (STA), a framework that allows reducing the duration of slow adiabatic processes [44,46–49], is believed to solve the above issue. It has been applied for fast and robust control of electron spin qubits in a single [50] and a double QD (DQD) [51,52], and for electron transfer in a long QD array [53,54]. Moreover, dynamical sweet spots have been investigated to increase the spin qubit decoherence time [55]. Also, nonadiabatic geometric phases, such as the Aharonov-Anandan phase [56], have been used to construct electron spin gates in semiconductor QDs [57,58] with reduced evolution time.

In this work, we propose a high-fidelity control protocol for the hole spin singlet-triplet qubit where both Rashba and Dresselhaus SOC play a prominent role. By fast quasiadiabatic (FAQUAD) approach [59], the detuning between energy levels $\varepsilon(t)$ is used as the control parameter so that the state evolution is along the adiabatic state as fast as possible, avoiding diabatic transitions. We compare the results obtained by FAQUAD and other protocols, such as a linear ramp, the LZ protocol, a π pulse, and

*gplatero@icmm.csic.es

a reduced version of FAQUAD known as local adiabatic (LA). Each of them may exhibit its advantages depending on the working scenario. However, we show that the proposed FAQUAD protocol for quantum control of a hole spin qubit allows achieving higher fidelities. Initializing the qubit at an arbitrary state, hole spin one-qubit and two-qubit gates such as CNOT and SWAP gates, achieve fidelities beyond the fault-tolerance error-correction threshold of 0.99 [60–62]. There are no other proposals in the literature for the design of two-qubit gates for hole spin singlet-triplet qubits. In this work, we focus on GaAs QDs where both Rashba and Dresselhaus interactions are present. However, the theoretical framework is general and therefore applicable to other materials such as Si or Ge where only Rashba SOC is present.

II. MODEL

We consider a planar DQD populated with two heavy holes (HHs), Fig. 1(a). The total Hamiltonian can be written as $H_0 = H_{\text{DQD}} + H_B + H_{\text{SOC}}$, where the first term reads

$$H_{\text{DQD}} = \sum_{i=L,R} \varepsilon_i c_i^\dagger c_i + U \sum_{i=L,R} n_{i\uparrow} n_{i\downarrow}$$
$$- t_N \sum_{\sigma=\uparrow,\downarrow} (c_{L\sigma}^\dagger c_{R\sigma} + \text{H.c.}). \quad (1)$$

Here ε_i with $i = L, R$ is the energy level of the left and right dots, respectively, U is the intradot Coulomb energy, and t_N the spin-conserving tunneling rate between adjacent dots. The operator $c_{i\sigma}$ ($c_{i\sigma}^\dagger$) is the annihilation (creation) of a hole state with spin σ in the dot i. The applied magnetic field with intensity B, perpendicular to the dots' plane, results in a Zeeman splitting $H_B = \frac{1}{2} g^* \mu_B B \sum_{i=L,R} (n_{i\uparrow} - n_{i\downarrow})$, where g^* is the effective Landé factor ($g^* = 1.45$ for holes in GaAs) and μ_B the Bohr magneton. Here we assume a homogeneous magnetic field and g factor, while
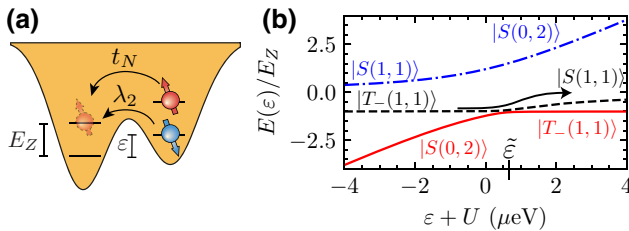

FIG. 1. (a) Scheme of a DQD populated with two holes with level detuning ε. t_N is the spin-conserving tunneling rate between dots, while the spin-flip tunneling rate λ_2 is a consequence of the SOC. The magnetic field perpendicular to the dots' plane produces a Zeeman splitting E_Z. (b) Energy-level diagram of the system. Basis states at large and low detunings are indicated. The $S - T_-$ anticrossing is located at $\tilde{\varepsilon}$. $B = 15$ mT, $U = 2$ meV, $t_N = 1$ μeV, $\lambda_2 = 0.1$ μeV.

the effect of an inhomogeneous g factor is analyzed in the Supplemental Material [63]. Finally, SOC is given by the term

$$H_{\text{SO}} = i\alpha E_\perp (\sigma_+ p_-^3 - \sigma_- p_+^3)$$
$$- \beta(\sigma_+ p_- p_+ p_- + \sigma_- p_+ p_- p_+). \quad (2)$$

The ladder operators are defined as $\sigma_\pm = (\sigma_x \pm i\sigma_y)/\sqrt{2}$, the momentum operator $p_\pm = p_x \pm i p_y$ given by $\vec{p} = -i\hbar\vec{\nabla} + e^*/c\vec{A}$, with e^* the hole effective electric charge, c the speed of light, and $\vec{A}$ the magnetic vector potential. Equation (2) represents the Rashba SOC (α) due to the structure inversion asymmetry, controlled by the effective electric field $E_\perp$ produced by the accumulation gate, and Dresselhaus SOC (β) due to the bulk inversion asymmetry. SOC in two-dimensional hole gases was analyzed in III-V and Si-based heterojunctions in Ref. [64], where it was shown that higher-order terms in the wave vector contained in the heavy-hole spin splitting are sizable. In GaAs QDs, cubic Rashba and Dresselhaus SOC are the dominant terms, while in systems like Ge and Si nanowires and elongated QDs, the spin orbit is modeled by the direct Rashba SOC [65,66]. Furthermore, depending on the QD configuration, linear contributions to the SOC could be relevant [67–70]. Nevertheless, in all these cases SOC can be included in a phenomenological model as a spin-flip term.

Since we consider a closed system, it is appropriate to work within the molecular basis of singlets: $|S(1,1)\rangle \equiv (|\uparrow,\downarrow\rangle - |\downarrow,\uparrow\rangle)/\sqrt{2}$, $|S(0,2)\rangle \equiv |0,\uparrow\downarrow\rangle$, and $|S(2,0)\rangle \equiv |\uparrow\downarrow,0\rangle$, and triplets $|T_0(1,1)\rangle \equiv (|\uparrow,\downarrow\rangle + |\downarrow,\uparrow\rangle)/\sqrt{2}$, $|T_-(1,1)\rangle \equiv |\downarrow,\downarrow\rangle$ and $|T_+(1,1)\rangle \equiv |\uparrow,\uparrow\rangle$. We write the spin-flip tunneling matrix element between the polarized triplet states and the double-occupied singlet state as $\langle T_\pm(1,1)| H_{\text{SOC}} |S(0,2)\rangle = \lambda_2$, and $\langle T_\pm(1,1)| H_{\text{SOC}} |S(1,1)\rangle = 2\lambda_2 S/\sqrt{2} = \lambda_1$ for the single-occupied singlet state. Here we define the overlap between the wave functions in each dot as $S \equiv \langle L|R\rangle = \exp(-d^2/2l^2)$, where d is the distance between dots, and l the extent of the wave function centered at each dot. The matrix element λ_2 also depends on these two parameters. The explicit expression showing this dependence is given in the Supplemental Material [63]. With the experimental parameters for GaAs QDs proposed in Ref. [20], we obtain the relation $\lambda_1/\lambda_2 \sim 1/100$.

Under a constant magnetic field B the unpolarized triplet state $|T_0(1,1)\rangle$ does not interact with any other state. The anticrossing between $|T_+(1,1)\rangle$ and the singlet states is located in a detuning $\varepsilon \equiv \varepsilon_R - \varepsilon_L$ close to $\varepsilon + U \sim -2t_N^2/E_Z + E_Z$. As we see below, our working regime is far from this detuning so $|T_+(1,1)\rangle$ does not interact with other states in our case, and we can neglect its contribution. Furthermore, if the detuning is large enough ($\varepsilon > -U$) the double-occupied singlet state $|S(2,0)\rangle$ is far apart in energy and does not play any role. Then, we write

the matrix form of the total Hamiltonian H_0 in the basis $(|T_-(1,1)\rangle, |S(0,2)\rangle, |S(1,1)\rangle)$ as

$$H_0 = \begin{pmatrix} -E_Z & \lambda_2 & \lambda_1 \\ \lambda_2^* & \varepsilon + U & -\sqrt{2}t_N \\ \lambda_1^* & -\sqrt{2}t_N & 0 \end{pmatrix}, \qquad (3)$$

with the Zeeman splitting in each dot E_Z, and $\varepsilon_L + \varepsilon_R = 0$. The instantaneous eigenenergies are shown in Fig. 1(b). Due to the finite spin-conserving tunneling rate t_N, the singlets form hybridized states

$$|S_G\rangle = \cos \Omega/2 \, |S(1,1)\rangle + \sin \Omega/2 \, |S(0,2)\rangle,$$
$$|S_E\rangle = -\sin \Omega/2 \, |S(1,1)\rangle + \cos \Omega/2 \, |S(0,2)\rangle, \quad (4)$$

where $\tan \Omega = 2\sqrt{2}t_N/(\varepsilon + U)$. We encode our computation basis with the triplet state and the ground hybridized singlet state. However, the transition between the charge configurations $(1,1)$ and $(0,2)$, leads to charge fluctuation. This is why we try to reduce the population of $|S(0,2)\rangle$ as much as possible. The anticrossing between singlet states is located at $\varepsilon + U = 0$. Far from this point, for $\varepsilon + U \gg t_N$, the ground hybridized singlet state is $|S_G\rangle \sim |S(1,1)\rangle$. It is this regime in which we are interested since charge noise is significantly reduced. The anticrossing between the triplet and the ground hybridized singlet state is located at $\tilde{\varepsilon} + U \sim 2t_N^2/E_Z - E_Z$. Then, we need that this anticrossing fulfills $\tilde{\varepsilon} + U \gg t_N$, which is verified in the limit $t_N \gg E_Z$, being this configuration the ideal one to avoid a significant contribution of $|S(0,2)\rangle$. The typical value for the spin-conserving tunneling rate is close to $t_N \sim 5$ μeV, while a reasonable magnetic field of $B \sim 5$ mT corresponds to a Zeeman spiting $E_Z \sim 0.4$ μeV, verifying the above condition. In particular, if $t_N > E_Z/\sqrt{2}$ the anticrossings between the singlet state and the triplet states $|T_-(1,1)\rangle$ and $|T_+(1,1)\rangle$ are far apart from each other, so the approximation of neglecting $|T_+(1,1)\rangle$ is justified. If other excited states are close to the working point, more elaborate protocols should be used to maintain high fidelity in the operations to avoid a possible leakage out of the computation basis. In particular, the speed of the protocol will be reduced in order to avoid transitions to these states.

III. TRANSFER $S(1,1) - T_-(1,1)$

We investigate the design of a detuning pulse in order to pass from $|T_-(1,1)\rangle$ to $|S(1,1)\rangle$ along the instantaneous state $|\phi_1\rangle$, where $H_0 |\phi_1(\varepsilon)\rangle = E_1(\varepsilon) |\phi_1(\varepsilon)\rangle$, whose instant eigenenergy $E_1(\varepsilon)$ is represented by the dashed black line in Fig. 1(b). There are different approaches to design the detuning pulse between the dots, the only driving parameter in our case. A linear ramp of the detuning between the initial and final time gives the adiabatic evolution when the time derivative of the detuning, i.e., the driving speed, is small enough $(\varepsilon(t_f) - \varepsilon(0))/t_f \ll \lambda_2$ so the adiabatic

condition is fulfilled during the protocol. To reduce the total time, one can consider an LZ-type protocol composed of a linear ramp with total time t_{raise}, a waiting time t_w, and another linear ramp returning to the original point. The total time of the protocol is given by $t_f = 2t_{\text{raise}} + t_w$. During the waiting time, the state acquires a phase interfering destructively or constructively during the returning linear ramp, resulting in a complete transfer. Another proposal for quantum control is the π pulse. In this protocol, all the parameters of the system are constant over time, with the detuning fixed at the anticrossing $\tilde{\varepsilon}$. By changing the total time of the protocol, the system undergoes Rabi oscillations between both states. If the waiting time is a multiple of $\pi/\hbar f(\lambda_2)$, where $f(\lambda_2)$ is the SOC energy gap, a transfer between states is achieved. However, this protocol works only properly when the system can be effectively reduced to a two-level system. If not, multiple π pulses must be employed in each of the anticrossings [71]. In this work, we propose to use a protocol, not yet experimentally implemented in semiconductor quantum dots, based on shortcuts to adiabaticity, in order to improve the fidelity of the established protocols mentioned above.

We investigate the FAQUAD [59] protocol, which efficiently allows the transfer to be sped up far from the anticrossings where diabatic transitions to excited states have a very low probability, and reduce the speed otherwise. The adiabaticity condition for a N-level system can be written as

$$c = \hbar \sum_{k \neq i}^{N} \left| \frac{\langle \phi_i(t)| \partial_t H(t) |\phi_k(t)\rangle}{[E_i(t) - E_k(t)]^2} \right|, \qquad (5)$$

where $|\phi_k(t)\rangle$ are the instantaneous eigenstates and $E_k(t)$ the corresponding eigenenergies. The system is initialized in the eigenstate given by $|\Psi(0)\rangle = |\phi_i(0)\rangle$. If the dynamics is slow enough, that is, $c \ll 1$, at the end of the protocol the system will remain in the same eigenstate $|\Psi(t_f)\rangle = |\phi_i(t_f)\rangle$. We assume that the system is driven by a single parameter, named ε, so we can write $\partial_t H = \dot{\varepsilon} \partial_\varepsilon H$, with $\dot{\varepsilon} \equiv \partial_t \varepsilon$ the driving speed. Imposing boundary conditions for the driving parameters (see below) we can rewrite the adiabatic condition in Eq. (5) as

$$c = \frac{\hbar}{t_f} \sum_{k \neq i}^{N} \int_{\varepsilon(0)}^{\varepsilon(t_f)} d\varepsilon \left| \frac{\langle \phi_i(\varepsilon)| \partial_\varepsilon H(t) |\phi_k(\varepsilon)\rangle}{[E_i(\varepsilon) - E_k(\varepsilon)]^2} \right|. \qquad (6)$$

The above integral has no analytical solution for a general system. However, it can be easily solved by numerical methods. Once the value of the adiabatic constant c is known, we can solve the following differential equation to obtain the time-dependent driving parameter:

$$\dot{\varepsilon} = \frac{c}{\hbar} \sum_{k \neq i}^{N} \left| \frac{[E_i(\varepsilon) - E_k(\varepsilon)]^2}{\langle \phi_i(\varepsilon)| \partial_\varepsilon H(t) |\phi_k(\varepsilon)\rangle} \right|. \qquad (7)$$

The solution of the above equation gives as a result a driving parameter that ensures a constant value of c during the transfer. The dynamic evolves fast if the control parameter is far from the avoided anticrossings, where no diabatic transitions are possible. Near the anticrossings, the driving slows down to ensure the adiabatic condition, staying in the instantaneous eigenstate, Fig. 2(a). We define the fidelity of the protocol as the total population of the single occupied singlet state at the final time $\mathcal{F} \equiv |\langle S(1,1)|\Psi(t_f)\rangle|^2$. In Fig. 2(b) we show how the fidelity depends on the total time of the protocol. As t_f increases the dynamic is closer to the adiabatic regime, i.e., $c \ll 1$. The characteristic of the FAQUAD protocol is the ondulatory behavior of fidelity, tending asymptotically to the value of unity. We define the first peak in the fidelity as $\tilde{\mathcal{F}}$, which is reached with a total time of $\tilde{t}_f$.

The boundary conditions for the driving parameter have a significant effect on the final result of the transfer. We start the dynamics initializing the system in the triplet state $|\Psi(t=0)\rangle = |T_-(1,1)\rangle$. However, this state does not exactly correspond to an instant eigenstate $|\phi_i\rangle$ with $|\langle T_-(1,1)|\phi_i(\varepsilon(0))\rangle|^2 = 1 - \gamma_0$ for $0 < \gamma_0 < 1$. Ideally, the protocol would start with a detuning such that $\gamma_0 = 0$, but this is only possible at the limit $\varepsilon(0) \rightarrow -\infty$. Then, working with a moderate value of $\varepsilon(0)$, γ_0 acquires a finite value. The same discussion is valid for the final

detuning at which $|\langle S(1,1)|\phi_i(\varepsilon(t_f))\rangle|^2 = 1 - \gamma_f$, but now the value of $\gamma_f = 0$ is only reached in the limit of large detuning $\varepsilon(t_f) \rightarrow \infty$. We study the dependence of $\tilde{\mathcal{F}}$ on the value of the boundary conditions fixing $\gamma_0 = \gamma_f$. In Fig. 2(c) we plot the infidelity at the first peak versus the detuning $\Delta\varepsilon \equiv \varepsilon(t_f) - \varepsilon(0)$. As we increase the range of detuning, the values of γ_0 and γ_f decrease, resulting in higher transfer fidelity. We find that the fidelity increases exponentially with the detuning range. Using a large detuning range is a promising way to achieve ultrahigh transfer fidelities. Furthermore, the total time needed to reach the first peak remains nearly constant when increasing the detuning range (not shown here). During the rest of the paper, we fix the boundary conditions such that $\gamma_0 = \gamma_f = 0.01$, obtaining a moderate value for the detuning $\Delta\varepsilon \sim 30~\mu$eV.

Besides the detuning range, a worthwhile thing to keep in mind for a possible experimental implementation is the pulse shape. With FAQUAD we obtain a control parameter pulse shape with sharp edges at both the beginning and the end of the protocol. In order to mimic a pulse that could be experimentally implemented, we divide the ideal pulse shape for the detuning into a series of linear ramps with an individual duration of Δt, see Fig. 3(a). The pulse is then divided into a total of $t_f/\Delta t$ linear ramps, recovering the ideal pulse at $\Delta t = 0$. In Fig. 3(b) we plot the fidelity for the $|T_-(1,1)\rangle \rightarrow |S(1,1)\rangle$ transfer versus the total time of the protocol using the ideal pulse, along with more realistic pulses with different time resolution Δt. In all cases, the maximum fidelity is $\mathcal{F} > 0.99$, even for values as high as $\Delta t = 20$ ns. We demonstrate that the pulses obtained with FAQUAD are robust against a finite time resolution of the control parameter, being a potential candidate for the manipulation of spin qubits in semiconductor QDs.
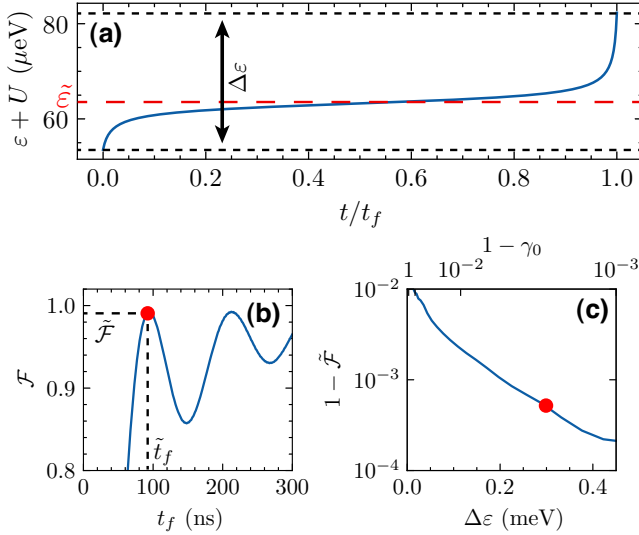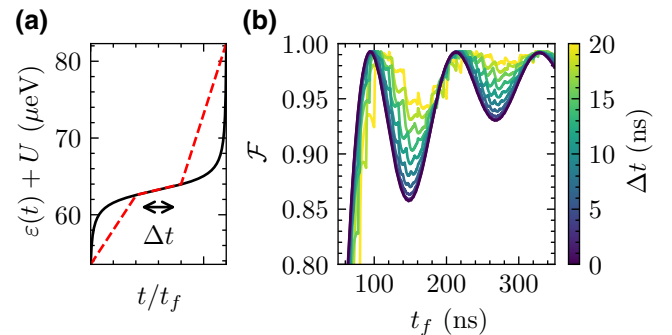

FIG. 2. (a) Detuning pulse shape obtained with FAQUAD. The boundary conditions for the detuning define the detuning range as $\Delta\varepsilon = \varepsilon(t_f) - \varepsilon(0)$. The dashed red line marks the location of the anticrossing. (b) Fidelity of the $|T_-(1,1)\rangle \rightarrow |S(1,1)\rangle$ transfer versus the total time of the protocol. The red dot marks the first peak in the fidelity $\tilde{\mathcal{F}}$, which is obtained for a total time of $\tilde{t}_f$. The detuning range used is $\Delta\varepsilon = 0.3$ meV. (c) Infidelity of FAQUAD versus the detuning range $\Delta\varepsilon$. The red dot corresponds to the fidelity shown in (b). $B = 10$ mT, $U = 2$ meV, $t_N = 5~\mu$eV, $\lambda_2 = 0.1~\mu$eV, $\lambda_1 = \lambda_2/100$.

FIG. 3. (a) Ideal pulse shape (solid black line), and a discretized pulse with certain time resolution Δt. (b) Fidelity for the $|T_-(1,1)\rangle \rightarrow |S(1,1)\rangle$ transfer with FAQUAD against the total time of the protocol for different values of the time resolution Δt. The limit $\Delta t \rightarrow 0$ (darker colors) denotes the limits of the ideal pulse. $g = 1.35$, $B = 10$ mT, $t_N = 5~\mu$eV, $\lambda_2 = 0.1~\mu$eV, and $U = 2$ meV.

A simplified version of FAQUAD known as local adiabatic [63,72,73] also gives rise to outstanding results. This protocol requires less information about the system if in Eq. (5) the next condition $\langle \phi_i(t)| \, \partial_t H(t) \, |\phi_k(t)\rangle = 1$, $\forall k \neq i$, is considered. This assumption, even if not verified at all times, highly simplifies the protocol, which no longer needs information about the eigenstates. It could be beneficial for its implementation where a precise characterization of all the parameters can be challenging (see the Supplemental Material [63] for more details). Furthermore, the fidelity obtained with this protocol is comparable to the results obtained with FAQUAD. Figure 4(a) shows the pulse derived from each of the mentioned protocols. Among all protocols, the highest fidelity is obtained by FAQUAD and LA, with the maximum value $\mathcal{F}_{\max} = 0.993$ [Fig. 4(b)]. FAQUAD reaches this value at a smaller t_f than LA, while the latter is less sensitive to a deviation in the final time t_f. Using a π pulse, we observe typical Rabi oscillations, but with $\mathcal{F} < 0.99$ at all final times. To understand the low fidelity obtained by performing a linear protocol, we can assume that we have a two-level system and that we can apply the Landau-Zener formula $\mathcal{F}^{\mathrm{LZ}} = 1 - \exp(-2\pi\lambda_2^2/\hbar\nu)$, where $\nu = \Delta\varepsilon/t_f$ is the speed of the linear ramp. We find that the detuning range is proportional to the spin-conserving tunneling rate $\Delta\varepsilon \propto t_N$. Using experimental parameters for HH in GaAs the SOC $\lambda_2/t_N = 0.02$ [74] is small. Using these parameters in the Landau-Zener formula we obtain low fidelity even for large times $\mathcal{F}^{\mathrm{LZ}}(t_f = 250 \text{ ns}) \sim 0.6$. This value is close to that obtained by numerical methods for the linear ramp [Fig. 4(b), orange line]. Applying a protocol consisting of two linear pulses plus a waiting time in between

substantially improves the results of a linear ramp. However, the maximum fidelity obtained with this pulse is still below the proposed FAQUAD protocol, which proves to be a better alternative than those protocols usually considered in experiments. Since the best results for state transfer are obtained with FAQUAD, we focus on this protocol and compare its feasibility with the other established ones.

In order to study the effect of the charge noise on the state transfer, we solve the master equation $\dot{\rho} = -i/\hbar[H_0, \rho] + \sum_i \left(L_i \rho L_i^\dagger - 1/2 \left\{ L_i^\dagger L_i, \rho \right\} \right)$, where the Lindblad operator is given by $L_i = (\sqrt{\Gamma_{\mathrm{ch}}} + \sqrt{\Gamma_{\mathrm{SD}}})\sigma_i$, and σ_i are the two diagonal Gell-Mann matrices. Pure dephasing is mainly caused by charge noise when $|S(0,2)\rangle$ is populated during the transfer. It leads to a dephasing strength $\Gamma_{\mathrm{ch}}(\varepsilon) = \gamma_2|\langle S(0,2)|\phi_1(\varepsilon)\rangle|^2$ [45]. Furthermore, we also include an extra spin-dephasing term (Γ_{SD}) due to the spin-orbit mixing of the HH states interacting with phonons [15], and to the hyperfine interaction. This spin-dephasing term is assumed to be constant at all detuning. Figures 5(a) and 5(b) show the fidelity of FAQUAD in terms of t_f and E_Z in the presence of charge noise and spin dephasing. In the limit of a large magnetic field, the total time needed to reach the first peak in the fidelity is much smaller than the spin-dephasing strength $\tilde{t}_f \ll 1/\Gamma_{\mathrm{SD}}$. However, the crossing between the singlet and the triplet states is located at $\tilde{\varepsilon} + U < 0$. In this region the ground state $|S_G\rangle \sim |S(0,2)\rangle$ and charge noise during the dynamics is the dominant noise source. The large population of $|S(0,2)\rangle$ results in low transfer fidelities. In the other limit, working with low magnetic fields, the relevance of $|S(0,2)\rangle$ decreases, while the total time $\tilde{t}_f$ that is needed to obtain a complete state transfer increases. Even if charge noise is highly suppressed in this limit, $\tilde{t}_f$ is high enough such that spin dephasing is relevant, resulting in
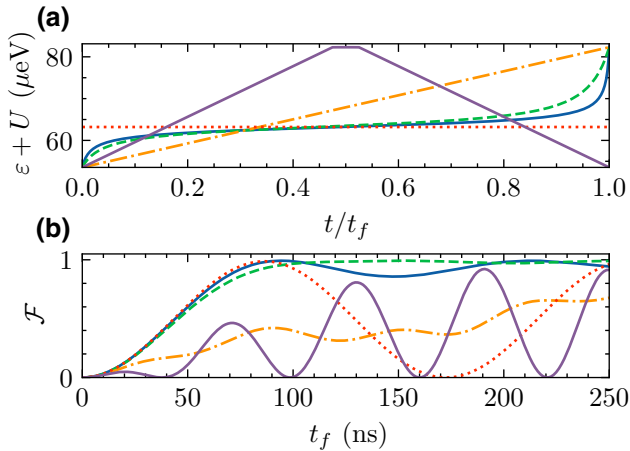

FIG. 4. (a) Pulse shapes for the state transfer $T_-(1,1) \rightarrow S(1,1)$, designed by FAQUAD (solid blue), LA (dashed green), linear (dotted-dashed orange), π pulse (dotted red), and the LZ-type protocol consisting in two linear ramps and a waiting time (solid purple). (b) Fidelity for the different protocols against the total time. $B = 10$ mT, $U = 2$ meV, $t_N = 5 \,\mu$eV, $\lambda_2 = 0.1 \,\mu$eV, $\lambda_1 = \lambda_2/100$, and $t_w = 0.05 t_{\mathrm{raise}}$.
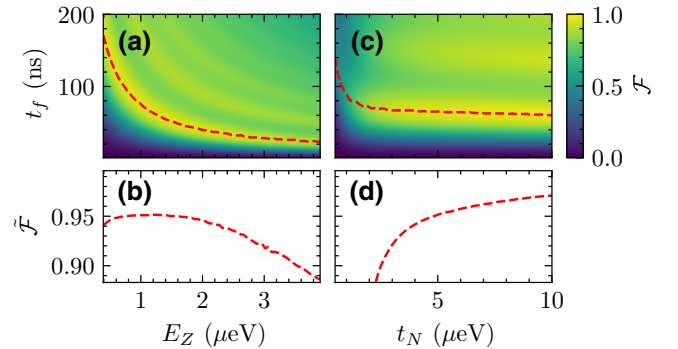

FIG. 5. (a),(c) Fidelity, considering the FAQUAD protocol, for the transfer $|T_-(1,1)\rangle \rightarrow |S(1,1)\rangle$ in the presence of charge noise and spin dephasing as a function of (a) E_Z and t_f with $t_N = 5 \,\mu$eV; (c) t_N and t_f with $E_Z = 1.17 \,\mu$eV. (b),(d) $\tilde{\mathcal{F}}$ corresponding to the dashed red lines shown in (a),(c). $U = 2$ meV, $\lambda_2 = 0.02 t_N$, $\lambda_1 = \lambda_2/100$, $\gamma_2 = 10^{-2}$ ns^{-1}, $\Gamma_{\mathrm{SD}} = 10^{-4}$ ns^{-1}.

a decrease of the fidelity $\tilde{\mathcal{F}}$. Therefore, there is a compromise between these two limits for the magnetic field intensity. With the parameters considered, the maximum fidelity is obtained at $B \sim 15$ mT, i.e., $E_Z \sim 1.17$ μeV. This value corresponds to the optimal point of operation for the state transfer.

We also analyze the dependence of $\mathcal{F}$ on the spin-conserving tunneling rate, Figs. 5(c) and 5(d) in the presence of charge noise and spin dephasing. Here we fix the ratio between the spin-flip and spin-conserving tunneling rates at $\lambda_2/t_N = 0.02$. As the tunneling rate increases, the crossing point moves farther from $\tilde{\varepsilon} + U = 0$, so that the ground hybrid singlet state is given by $|S_G\rangle \sim |S(1,1)\rangle$. Then, $|S(0,2)\rangle$ is not populated during the transfer resulting in low charge noise. In this case, increasing t_N has low effect on the total time $\tilde{t}_f$. However, working with large t_N results in an increase of the detuning range $\Delta\varepsilon \equiv \varepsilon(t_f) - \varepsilon(0)$ needed to obtain the same boundary condition of γ_0 and γ_f. If the initial of the final detuning is high enough, surpassing the lead barriers, new particles can enter the system, modifying the results shown here. Therefore, for a practical scenario in an experimental device, a moderate t_N is required.

IV. QUBIT-STATE INITIALIZATION

One of DiVincenzo's criteria for the construction of a quantum computer [75] is the ability to initialize the state of the qubit. We use the singlet-triplet states to map the computational basis as $|0\rangle \equiv |T_-(1,1)\rangle$ and $|1\rangle \equiv |S(1,1)\rangle$. A general qubit state is written as

$$|\Psi\rangle = \cos\theta/2 \, |T_-(1,1)\rangle + e^{i\phi}\sin\theta/2 \, |S(1,1)\rangle, \quad (8)$$

where θ and ϕ are the polar and azimuthal angles, respectively, defined on the Bloch sphere. To achieve a general state, the qubit is first initialized at $|T_-(1,1)\rangle$ using spin-selective operations on the DQD system. Another possibility of initialization is to let the system decay to its ground state, which corresponds to $|T_-(1,1)\rangle$ in the limit $\varepsilon < \tilde{\varepsilon}$. Our goal is to develop a protocol that can be applied to evolve the system to an arbitrary value of the angles θ and ϕ. When performing a FAQUAD protocol, we find that varying t_f from $t_f \to 0$ to $t_f = \tilde{t}_f$, which corresponds to the first peak in the fidelity of the state transfer, the final polar angle goes smoothly from $\theta \to 0$ to $\theta \to \pi$. Then, the polar angle can be tuned by implementing a FAQUAD pulse with a given t_f that depends on the desired polar angle. The acquired azimuthal angle during the process of FAQUAD depends on the final polar angle, $\phi_{\text{FAQUAD}}(\theta_f)$, which can be approximated by a second-order polynomial function. To achieve the desired phase, one can do a rotation around the z axis by letting the system evolve in the large detuning limit. The phase during this waiting time t_w reads $\phi_w = 1/\hbar \int_0^{t_w} dt[E_{S(1,1)} - E_{T_-(1,1)}] = -E_z/\hbar t_w$. This
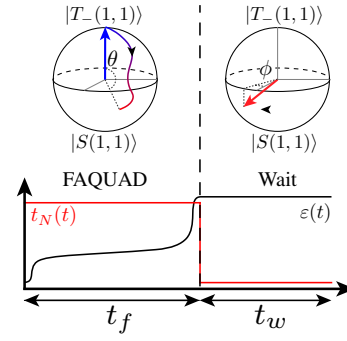

FIG. 6. Scheme for the state initialization protocol. The first step consists of a FAQUAD pulse in the detuning ε, obtaining the final polar angle θ. In the second step, the tunneling t_N is set to zero, and the system evolves acquiring a phase ϕ.

last expression is only valid if the coupling between the states is low enough, which can be obtained using large detuning, or simply turning off the tunneling rate and setting $t_N = 0$. The total phase after the waiting time is given by $\phi = \phi_{\text{FAQUAD}}(\theta) + \phi_w(t_w)$. From here we can extract t_w, which depends on both ϕ and θ. This protocol is schematically shown in Fig. 6.

V. NOT GATE

One of the main one-qubit gates in all quantum algorithms is the NOT gate (also known as the X gate), represented by the σ_x Pauli matrix. The action of this gate is a π rotation around the x axis. For instance, if the qubit is initialized in $|0\rangle$, after applying the NOT gate the qubit will be in the state $|1\rangle$, and vice versa. In our system, we can implement a NOT gate by applying FAQUAD with a total time $t_f = \tilde{t}_f$ and a waiting time t_w such that the dynamical phase is corrected, which is almost insensitive to the initial state. We define the fidelity of the NOT gate as $\mathcal{F}_{\text{NOT}} \equiv |\langle\Psi(0)| \sigma_x |\Psi(t_f)\rangle|^2$, which is shown in Fig. 7 for different initial states. The fidelity achieved for different initial polar angles (θ_0) and azimuthal angles (ϕ_0) is always $\mathcal{F}_{\text{NOT}} > 0.99$, and the corresponding gate time is 73.37 ns. The average fidelity for all possible initial states is $\mathcal{F}_{\text{NOT}} = 0.995$. Using other protocols such as LA or a π pulse lower fidelity is obtained. The results for these protocols are shown in the Supplemental Material [63].

VI. TWO-QUBIT GATES

Now we propose to implement a CNOT gate considering a linear array of two DQDs, as shown in Fig. 8(a). The system is described by the Hamiltonian $H_{2Q} = H_0^{(1)} + H_0^{(2)} + H_{\text{int}}$, where $H_0^{(1,2)}$ are the single-qubit Hamiltonians for each DQD [see Eq. (3)], and $H_{\text{int}} = -\sum_{\sigma,\sigma'=\{\uparrow,\downarrow\}} t_{\sigma,\sigma'} \left(c_{2\sigma}^\dagger c_{3\sigma'} + \text{h.c.}\right)$ is the coupling Hamiltonian between them, with $t_{\sigma,\sigma'} = t_N$ for $\sigma = \sigma'$, and
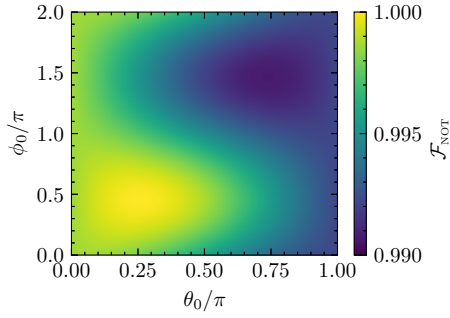
FIG. 7. Fidelity of the NOT gate implemented with FAQUAD, as a function of the initial state of the qubit defined by the polar angle θ_0 and the azimuthal angle ϕ_0. $B = 5$ mT, $U = 2$ meV, $t_N = 5 \, \mu$eV, $\lambda_2 = 0.25 \, \mu$eV, $\lambda_1 = \lambda_2/100$, FAQUAD time $\tilde{t}_f = 69.16$ ns, and waiting time $t_w = 4.21$ ns.

$t_{\sigma,\sigma'} = \lambda_2$ otherwise. Each qubit is defined by the singlet-triplet hole spin in the corresponding DQD. In this section, the hole spin states are labeled as $|S_{ij}\rangle$ and $|T_{ij}^-\rangle$ for the singlet and the triplet states, respectively, with one hole in each dot.

One DQD defines the target qubit on which a one-qubit gate will be performed, while the other DQD is the control qubit that governs whether the operation on the target qubit will be performed. If the control qubit is in the state $|0\rangle$, no operation applies to the target qubit, in other words, the identity gate is applied leaving the target qubit in its original state. On the other hand, if the control qubit is in the state $|1\rangle$, a NOT gate is performed to the target qubit. The CNOT gate reads $U_{\text{CNOT}} = |0\rangle\langle 0| \otimes \mathbb{1} + |1\rangle\langle 1| \otimes \sigma_x$.

In this case, the left-most DQD defines the target qubit, while the right-most DQD controls the two-qubit gate. The energy-level diagram against detuning between the two left-most dots is shown in Fig. 8(b), while the detuning between the two right-most dots remains constant. Due to the coupling between the middle dots, the $T_{12}^- - S_{12}$ avoided anticrossing location depends on the state of the control qubit. Tuning a FAQUAD protocol to work near the transition with the control qubit in the $|S_{34}\rangle$ state ($\varepsilon_{12} + U \sim 92 \, \mu$eV), the dynamics of the target qubit is
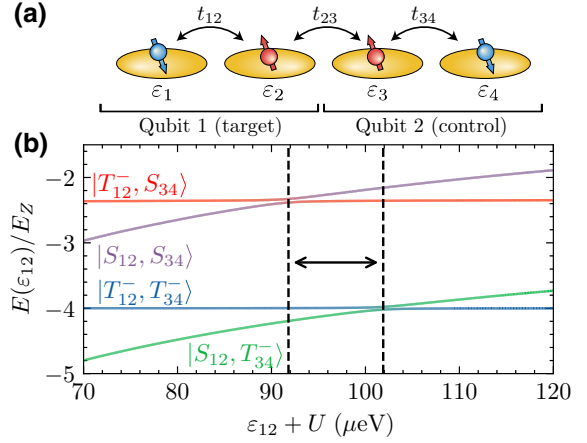

FIG. 8. (a) Scheme of a quadruple QD array populated with four HHs. Each pair represents one $|S\rangle$-$|T_-\rangle$ qubit. (b) Energy-level diagram versus the detuning between the two left-most quantum dots $\varepsilon_{12} \equiv \varepsilon_2 - \varepsilon_1$, while the detuning between the other dots is kept constant at $\varepsilon_{34} + U = 50 \, \mu$eV. $B = 2.3$ mT, $t_{N,12} = t_{N,34} = 10 \, \mu$eV, $t_{N,23} = 5 \, \mu$eV $t_{F,ij} = 0.02t_{N,ij}$, $U = 2$ meV.

reduced to the case of a single qubit, performing a NOT gate. However, using the same pulse with the control qubit in the $|T_{34}\rangle$ state, there is no anticrossing in the working detuning regime, so the target qubit remains in the same initial state since the dynamic is diabatic. It is the shift in energies between both anticrossings due to the coupling between the second and the third QDs that makes this protocol possible. The fidelity of the quantum gate will increase with the difference in detuning for each anticrossing. Furthermore, we can also tune the FAQUAD protocol to work near the other anticrossing ($\varepsilon_{12} + U \sim 102 \, \mu$eV), resulting in a quantum gate given by a NOT gate over the control qubit, a CNOT gate, and finally another NOT gate over the control qubit.

By tuning the total time of the protocol and the magnetic field intensity, we have control over the acquired phases. Setting the total time of the FAQUAD protocol to $t_f = 182.73$ ns, and a waiting time of $t_w = 5.6$ ns, the gate applied corresponds to a pure CNOT. The explicit value of the unitary transformation at the given total time is

$$
U_{\text{CNOT}}(t_f) = \begin{pmatrix} 1 & 0.05 + 0.02i & 0.01 & 0.02 \\ -0.05 + 0.02i & 0.99 & -0.05 + 0.01i & 0.05 - 0.01i \\ -0.01 & -0.05 & -0.03 & 0.99 - 0.12i \\ -0.01 & 0.05 + 0.01i & 0.99 + 0.08i & 0.03 \end{pmatrix}
\begin{matrix} |0,0\rangle \\ |1,0\rangle \\ |0,1\rangle \\ |1,1\rangle \end{matrix} \tag{9}
$$

To compute the fidelity of the two-qubit gate we use [76,77]

$$\mathcal{F}_{2Q} = \frac{1}{d(d+1)} \left[\text{Tr} \left(MM^\dagger \right) + |\text{Tr}(M)|^2 \right], \quad (10)$$

where $d = 4$ is the dimension of the computational space and $M \equiv U_{\text{tar}}^\dagger U(t_f)$ with U_{tar} the target unitary evolution matrix, i.e., the NOT gate defined above. Using our proposed protocol we obtain a CNOT gate fidelity of $\mathcal{F}_{\text{CNOT}} = 0.99$. This two-qubit gate fidelity is comparable with other proposals, which use electrons instead of holes (see Ref. [39]).

For higher detuning values, near $\varepsilon_{12} \sim \varepsilon_{34}$ there is an anticrossing between $|S_{12}, T_{34}^-\rangle$ and $|T_{12}^-, S_{34}\rangle$, see Fig. 9(b). By applying FAQUAD at this avoided anticrossing we can achieve a SWAPlike gate. A pure SWAP gate is a two-qubit gate that interchanges the states of two qubits. We refer to SWAPlike when nonzero phases are allowed for nondiagonal elements. SWAP gates are also one of the most used two-qubit gates for implementing quantum algorithms since it allows distant qubits to be coupled by sequentially transferring the quantum information between neighboring dots

$$U_{\text{SWAPlike}} = \begin{pmatrix} 1 & 0 & 0 & 0 \\ 0 & 0 & e^{\varphi_1} & 0 \\ 0 & e^{\varphi_2} & 0 & 0 \\ 0 & 0 & 0 & 1 \end{pmatrix}. \quad (11)$$

Using a FAQUAD pulse during a total of $t_f = 38$ ns, we obtain the following evolution matrix:

$$U_{\text{SWAP}}(t_f) = \begin{pmatrix} 1 & -0.015 - 0.02i & -0.004 + 0.002i & 0 \\ 0.003 - 0.005i & 0.061 - 0.051i & -0.011 - 0.996i & -0.008 + 0.011i \\ 0.015 - 0.001i & 0.993 + 0.082i & -0.055 + 0.057i & -0.007 \\ 0 & 0.008 & 0.011 - 0.008i & 0.999 \end{pmatrix}. \quad (12)$$

We can see that the obtained two-qubit gate corresponds to a SWAP gate with some additional phases in the off-diagonal matrix elements. However, a pure SWAP gate can be recovered with two additional local gates on each qubit. The fidelity obtained with FAQUAD is $\mathcal{F}_{\text{SWAP}} = 0.995$, beyond the error-correction threshold. In Fig. 9(b) we compare the fidelity of the SWAP gate for different protocols against charge noise. This noise source is modeled as a pure dephasing mechanism whose strength is proportional to the population of the double-occupied state. Here the average gate fidelity is defined using the Haar measure over the quantum states of two qubits [78]. We find that the linear ramp is very sensitive to charge noise, since the total time needed for the gate $t_f \sim 69$ ns is much larger than for the other three protocols, FAQUAD, LA, and a π pulse, with $t_f \sim 38$ ns. A detailed discussion on the effect of systematic and stochastic errors on ε_{12} and $t_{N,12}$ can be found within the Supplemental Material [63].

The parameters used in this section are selected such that high-fidelity quantum gates are obtained. However, a more exhaustive analysis can be performed to find even higher fidelities. This detailed exploration can be obtained with the help of numerical methods such as gradient-descent algorithms, which explore the multidimensional space spanned by the different parameters of the system, e.g., the tunneling rates, the magnetic field intensity, or the detuning between dots 3 and 4. However, this analysis is beyond the scope of this work.
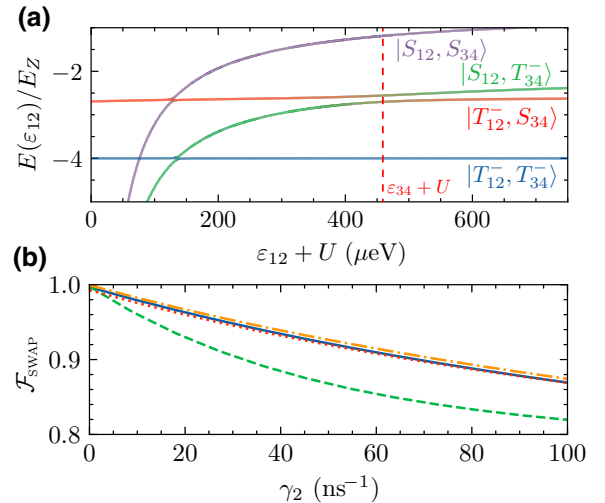

FIG. 9. (a) Energy-level diagram versus the detuning between the two left-most QDs $\varepsilon_{12} \equiv \varepsilon_2 - \varepsilon_1$. The colors represent the population of the basis states in each instantaneous eigenstate. (b) Fidelity of the SWAP gate obtained with FAQUAD (solid blue), linear (dashed green), π pulse (dotted dashed orange), and LA (dotted red) as a function of charge noise. $\varepsilon_{34} + U = 459$ μeV, $B = 5$ mT, $t_{N,12} = t_{N,34} = 10$ μeV, $t_{N,23} = 4.8$ μeV, $\lambda_{2,ij} = 0.02 t_{N,ij}$, $U = 2$ meV. The protocol times are $(38, 69, 37, 39.6)$ ns and the waiting times are $(2.55, 2.46, 0.44, 1.16)$ ns for FAQUAD, linear, π pulse and LA, respectively.

VII. EXPERIMENTAL IMPLEMENTATION

During our work, we focus on the study of GaAs QDs. However, our analysis can be extended to other semiconducting materials, such as Si or Ge, where the main features of FAQUAD are still valid. It can be also implemented in materials that present an inhomogeneous g factor (see Supplemental Material [63]).

VIII. CONCLUSIONS

In this work, we propose a fast quasiadiabatic protocol to implement the S-T hole spin qubit transition in a DQD. As the dynamic follows the adiabatic trajectory in a fast way, we are able to highly decrease charge noise by reducing the population of the double-occupied singlet state as compared with other protocols. The reduced total time of the protocol also makes it robust against spin dephasing. By means of this all-electrical protocol, we can initialize the qubit in an arbitrary state with high fidelity. Furthermore, we are able to perform a single-qubit gate, a NOT gate, combining the FAQUAD pulse and a waiting period to account for additional phases. We extend our scheme to two DQDs, each DQD representing one qubit. Driving one of the qubits allows for a two-qubit gate, a CNOT gate with 0.99 of fidelity. We also propose how to implement a two-qubit SWAPlike gate, achieving a fidelity of 0.995. In both cases, the obtained fidelity is beyond the fault-tolerance error correction threshold. Finally, we compare the fidelity of different experimentally used protocols against the charge-noise strength.

Our results demonstrate the feasibility of the proposed protocol for the implementation of one- and two-hole spin qubit gates with high fidelity. These results are a step towards the logic gates' implementation with hole spin qubits in semiconductor quantum dots.

ACKNOWLEDGMENTS

[1] S. Tarucha, D. G. Austing, T. Honda, R. J. van der Hage, and L. P. Kouwenhoven, Shell Filling and Spin effects in a Few Electron Quantum Dot, Phys. Rev. Lett. **77**, 3613 (1996).

[2] D. Loss and D. P. DiVincenzo, Quantum computation with quantum dots, Phys. Rev. A **57**, 120 (1998).

[3] M. Ciorga, A. S. Sachrajda, P. Hawrylak, C. Gould, P. Zawadzki, S. Jullian, Y. Feng, and Z. Wasilewski, Addition spectrum of a lateral dot from Coulomb and spin-blockade spectroscopy, Phys. Rev. B **61**, R16315 (2000).

[4] R. Hanson, L. P. Kouwenhoven, J. R. Petta, S. Tarucha, and L. M. K. Vandersypen, Spins in few-electron quantum dots, Rev. Mod. Phys. **79**, 1217 (2007).

[5] C. Kloeffel and D. Loss, Prospects for spin-based quantum computing in quantum dots, Annu. Rev. Condens. Matter Phys. **4**, 51 (2013).

[6] M. Busl, G. Granger, L. Gaudreau, R. Sánchez, A. Kam, M. Pioro-Ladrière, S. A. Studenikin, P. Zawadzki, Z. R. Wasilewski, A. S. Sachrajda, and G. Platero, Bipolar spin blockade and coherent state superpositions in a triple quantum dot, Nat. Nanotechnol. **8**, 261 (2013).

[7] R. Sánchez, G. Granger, L. Gaudreau, A. Kam, M. Pioro-Ladrière, S. Studenikin, P. Zawadzki, A. Sachrajda, and G. Platero, Long-Range Spin Transfer in Triple Quantum Dots, Phys. Rev. Lett. **112**, 176803 (2014).

[8] J. Picó-Cortés, F. Gallego-Marcos, and G. Platero, Direct transfer of two-electron quantum states in ac-driven triple quantum dots, Phys. Rev. B **99**, 155421 (2019).

[9] M. Veldhorst, C. H. Yang, J. C. C. Hwang, W. Huang, J. P. Dehollain, J. T. Muhonen, S. Simmons, A. Laucht, F. E. Hudson, K. M. Itoh, A. Morello, and A. S. Dzurak, A two-qubit logic gate in silicon, Nature **526**, 410 (2015).

[10] A. M. J. Zwerver, *et al.*, Qubits made by advanced semiconductor manufacturing, Nat. Electron. **5**, 184 (2022).

[11] A. R. Mills, C. R. Guinn, M. J. Gullans, A. J. Sigillito, M. M. Feldman, E. Nielsen, and J. R. Petta, Two-qubit silicon quantum processor with operation fidelity exceeding 99%, Sci. Adv. **8**, eabn5130 (2022).

[12] M. T. Mądzik, S. Asaad, A. Youssry, B. Joecker, K. M. Rudinger, E. Nielsen, K. C. Young, T. J. Proctor, A. D. Baczewski, A. Laucht, V. Schmitt, F. E. Hudson, K. M. Itoh, A. M. Jakob, B. C. Johnson, D. N. Jamieson, A. S. Dzurak, C. Ferrie, R. Blume-Kohout, and A. Morello, Precision tomography of a three-qubit donor quantum processor in silicon, Nature **601**, 348 (2022).

[13] A. Noiri, K. Takeda, T. Nakajima, T. Kobayashi, A. Sammak, G. Scappucci, and S. Tarucha, Fast universal quantum gate above the fault-tolerance threshold in silicon, Nature **601**, 338 (2022).

[14] X. Xue, M. Russ, N. Samkharadze, B. Undseth, A. Sammak, G. Scappucci, and L. M. K. Vandersypen, Quantum logic with spin qubits crossing the surface code threshold, Nature **601**, 343 (2022).

[15] D. V. Bulaev and D. Loss, Spin Relaxation and Decoherence of Holes in Quantum Dots, Phys. Rev. Lett. **95**, 076805 (2005).

[16] D. Heiss, S. Schaeck, H. Huebl, M. Bichler, G. Abstreiter, J. J. Finley, D. V. Bulaev, and D. Loss, Observation of extremely slow hole spin relaxation in self-assembled quantum dots, Phys. Rev. B **76**, 241306 (2007).

[17] V. S. Pribiag, S. Nadj-Perge, S. M. Frolov, J. W. G. van den Berg, I. van Weperen, S. R. Plissard, E. P. A. M. Bakkers, and L. P. Kouwenhoven, Electrical control of single hole spins in nanowire quantum dots, Nat. Nanotechnol. **8**, 170 (2013).

[18] J. H. Prechtel, A. V. Kuhlmann, J. Houel, A. Ludwig, S. R. Valentin, A. D. Wieck, and R. J. Warburton, Decoupling a hole spin qubit from the nuclear spins, Nat. Mater. **15,** 981 (2016).

[19] A. Bogan, S. Studenikin, M. Korkusinski, G. Aers, L. Gaudreau, P. Zawadzki, A. Sachrajda, L. Tracy, J. Reno, and T. Hargett, Consequences of Spin-Orbit Coupling at the Single Hole Level: Spin-Flip Tunneling and the Anisotropic *g* Factor, Phys. Rev. Lett. **118,** 167701 (2017).

[20] A. Bogan, S. Studenikin, M. Korkusinski, L. Gaudreau, P. Zawadzki, A. S. Sachrajda, L. Tracy, J. Reno, and T. Hargett, Landau-Zener-Stückelberg-Majorana interferometry of a single hole, Phys. Rev. Lett. **120,** 207701 (2018).

[21] S. D. Liles, R. Li, C. H. Yang, F. E. Hudson, M. Veldhorst, A. S. Dzurak, and A. R. Hamilton, Spin and orbital structure of the first six holes in a silicon metal-oxide-semiconductor quantum dot, Nat. Commun. **9,** 3255 (2018).

[22] A. Bogan, S. Studenikin, M. Korkusinski, L. Gaudreau, P. Zawadzki, A. Sachrajda, L. Tracy, J. Reno, and T. Hargett, Single hole spin relaxation probed by fast single-shot latched charge sensing, Commun. Phys. **2,** 17 (2019).

[23] N. W. Hendrickx, W. I. L. Lawrie, L. Petit, A. Sammak, G. Scappucci, and M. Veldhorst, A single-hole spin qubit, Nat. Commun. **11,** 3478 (2020).

[24] N. W. Hendrickx, D. P. Franke, A. Sammak, G. Scappucci, and M. Veldhorst, Fast two-qubit logic with holes in germanium, Nature **577,** 487 (2020).

[25] P. M. Mutter and G. Burkard, Natural heavy-hole flopping mode qubit in germanium, Phys. Rev. Res. **3,** 013194 (2021).

[26] F. N. M. Froning, L. C. Camenzind, O. A. H. van der Molen, A. Li, E. P. A. M. Bakkers, D. M. Zumbühl, and F. R. Braakman, Ultrafast hole spin qubit with gate-tunable spin–orbit switch functionality, Nat. Nanotechnol. **16,** 308 (2021).

[27] F. van Riggelen, N. W. Hendrickx, W. I. L. Lawrie, M. Russ, A. Sammak, G. Scappucci, and M. Veldhorst, A two-dimensional array of single-hole quantum dots, Appl. Phys. Lett. **118,** 044002 (2021).

[28] N. W. Hendrickx, W. I. L. Lawrie, M. Russ, F. van Riggelen, S. L. de Snoo, R. N. Schouten, A. Sammak, G. Scappucci, and M. Veldhorst, A four-qubit germanium quantum processor, Nature **591,** 580 (2021).

[29] Z. Wang, E. Marcellina, A. R. Hamilton, J. H. Cullen, S. Rogge, J. Salfi, and D. Culcer, Optimal operation points for ultrafast, highly coherent Ge hole spin-orbit qubits, npj Quantum Inf. **7,** 54 (2021).

[30] K. Wang, G. Xu, F. Gao, H. Liu, R.-L. Ma, X. Zhang, Z. Wang, G. Cao, T. Wang, J.-J. Zhang, D. Culcer, X. Hu, H.-W. Jiang, H.-O. Li, G.-C. Guo, and G.-P. Guo, Ultrafast coherent control of a hole spin qubit in a germanium quantum dot, Nat. Commun. **13,** 206 (2022).

[31] C. Kloeffel, M. Trif, and D. Loss, Strong spin-orbit interaction and helical hole states in Ge/Si nanowires, Phys. Rev. B **84,** 195314 (2011).

[32] P. Szumniak, S. Bednarek, B. Partoens, and F. M. Peeters, Spin-Orbit-Mediated Manipulation of Heavy-Hole Spin Qubits in Gated Semiconductor Nanodevices, Phys. Rev. Lett. **109,** 107201 (2012).

[33] H. Watzinger, J. Kukučka, L. Vukušić, F. Gao, T. Wang, F. Schäffler, J.-J. Zhang, and G. Katsaros, A germanium hole spin qubit, Nat. Commun. **9,** 3902 (2018).

[34] L. Vukušić, J. Kukučka, H. Watzinger, J. M. Milem, F. Schäffler, and G. Katsaros, Single-shot readout of hole spins in Ge, Nano Lett. **18,** 7141 (2018).

[35] N. W. Hendrickx, D. P. Franke, A. Sammak, M. Kouwenhoven, D. Sabbagh, L. Yeoh, R. Li, M. L. V. Tagliaferri, M. Virgilio, G. Capellini, G. Scappucci, and M. Veldhorst, Gate-controlled quantum dots and superconductivity in planar germanium, Nat. Commun. **9,** 2835 (2018).

[36] F. N. M. Froning, M. J. Rančić, B. Hetényi, S. Bosco, M. K. Rehmann, A. Li, E. P. A. M. Bakkers, F. A. Zwanenburg, D. Loss, D. M. Zumbühl, and F. R. Braakman, Strong spin-orbit interaction and *g*-factor renormalization of hole spins in Ge/Si nanowire quantum dots, Phys. Rev. Res. **3,** 013081 (2021).

[37] A. Crippa, R. Maurand, L. Bourdet, D. Kotekar-Patil, A. Amisse, X. Jehl, M. Sanquer, R. Laviéville, H. Bohuslavskyi, L. Hutin, S. Barraud, M. Vinet, Y.-M. Niquet, and S. D. Franceschi, Electrical Spin Driving by *g*-Matrix Modulation in Spin-Orbit Qubits, Phys. Rev. Lett. **120,** 137702 (2018).

[38] H. Ribeiro and G. Burkard, Nuclear State Preparation via Landau-Zener-Stückelberg Transitions in Double Quantum Dots, Phys. Rev. Lett. **102,** 216802 (2009).

[39] H. Ribeiro, J. R. Petta, and G. Burkard, Harnessing the GaAs quantum dot nuclear spin bath for quantum control, Phys. Rev. B **82,** 115445 (2010).

[40] J. R. Petta, H. Lu, and A. C. Gossard, A coherent beam splitter for electronic spin states, Science **327,** 669 (2010).

[41] J. M. Nichol, S. P. Harvey, M. D. Shulman, A. Pal, V. Umansky, E. I. Rashba, B. I. Halperin, and A. Yacoby, Quenching of dynamic nuclear polarization by spin–orbit coupling in GaAs quantum dots, Nat. Commun. **6,** 7682 (2015).

[42] S. S. Gomez and R. H. Romero, Superadiabatic spin-preserving control of a single-spin qubit in a double quantum dot with spin–orbit interaction, J. Phys. B: At., Mol. Opt. Phys. **52,** 235502 (2019).

[43] A. D. Greentree, J. H. Cole, A. R. Hamilton, and L. C. L. Hollenberg, Coherent electronic transfer in quantum dot systems using adiabatic passage, Phys. Rev. B **70,** 235317 (2004).

[44] J. Huneke, G. Platero, and S. Kohler, Steady-State Coherent Transfer by Adiabatic Passage, Phys. Rev. Lett. **110,** 036802 (2013).

[45] H. Ribeiro, G. Burkard, J. R. Petta, H. Lu, and A. C. Gossard, Coherent Adiabatic Spin Control in the Presence of Charge Noise using Tailored Pulses, Phys. Rev. Lett. **110,** 086804 (2013).

[46] X. Chen, A. Ruschhaupt, S. Schmidt, A. del Campo, D. Guéry-Odelin, and J. G. Muga, Fast Optimal Frictionless Atom Cooling in Harmonic Traps: Shortcut to Adiabaticity, Phys. Rev. Lett. **104,** 063002 (2010).

[47] A. Ruschhaupt, X. Chen, D. Alonso, and J. G. Muga, Optimally robust shortcuts to population inversion in two-level quantum systems, New J. Phys. **14,** 093040 (2012).

[48] E. Torrontegui, S. Ibáñez, S. Martínez-Garaot, M. Modugno, A. del Campo, D. Guéry-Odelin, A. Ruschhaupt, X.

Chen, and J. G. Muga, in *Advances In Atomic, Molecular, and Optical Physics* (Elsevier, 2013), p. 117.

[49] Y.-C. Li, X. Chen, J. G. Muga, and E. Y. Sherman, Qubit gates with simultaneous transport in double quantum dots, New J. Phys. **20,** 113029 (2018).

[50] Y. Ban, X. Chen, E. Y. Sherman, and J. G. Muga, Fast and Robust Spin Manipulation in a Quantum Dot by Electric Fields, Phys. Rev. Lett. **109,** 206602 (2012).

[51] D. V. Khomitsky, L. V. Gulyaev, and E. Y. Sherman, Spin dynamics in a strongly driven system: Very slow Rabi oscillations, Phys. Rev. B **85,** 125312 (2012).

[52] Y. Ban and X. Chen, Counter-diabatic driving for fast spin control in a two-electron double quantum dot, Sci. Rep. **4,** 6258 (2014).

[53] Y. Ban, X. Chen, and G. Platero, Fast long-range charge transfer in quantum dot arrays, Nanotechnology **29,** 505201 (2018).

[54] Y. Ban, X. Chen, S. Kohler, and G. Platero, Spin entangled state transfer in quantum dot arrays: Coherent adiabatic and speed-up protocols, Adv. Quantum Technol. **2,** 1900048 (2019).

[55] J. Picó-Cortés and G. Platero, Dynamical second-order noise sweetspots in resonantly driven spin qubits, Quantum **5,** 607 (2021).

[56] Y. Aharonov and J. Anandan, Phase Change during a Cyclic Quantum Evolution, Phys. Rev. Lett. **58,** 1593 (1987).

[57] C. Zhang, T. Chen, S. Li, X. Wang, and Z.-Y. Xue, High-fidelity geometric gate for silicon-based spin qubits, Phys. Rev. A **101,** 052302 (2020).

[58] M.-Y. Chen, C. Zhang, and Z.-Y. Xue, Fast high-fidelity geometric gates for singlet-triplet qubits, Phys. Rev. A **105,** 022620 (2022).

[59] S. Martínez-Garaot, A. Ruschhaupt, J. Gillet, T. Busch, and J. G. Muga, Fast quasiadiabatic dynamics, Phys. Rev. A **92,** 043406 (2015).

[60] R. Raussendorf and J. Harrington, Fault-Tolerant Quantum Computation with High Threshold in Two Dimensions, Phys. Rev. Lett. **98,** 190504 (2007).

[61] D. S. Wang, A. G. Fowler, and L. C. L. Hollenberg, Surface code quantum computing with error rates over 1%, Phys. Rev. A **83,** 020302 (2011).

[62] A. G. Fowler, M. Mariantoni, J. M. Martinis, and A. N. Cleland, Surface codes: Towards practical large-scale quantum computation, Phys. Rev. A **86,** 032324 (2012).

[63] See Supplemental Material http://link.aps.org/supplemental/10.1103/PhysRevApplied.18.054090 for more details on how to obtain the effective Hamiltonian, an extensive study of the LA and LZ protocols, the effects of an anisotropic *g* factor, and the study of the SWAP gate fidelity under systematic and stochastic noises. This material includes Refs. [79–82].

[64] E. Marcellina, A. R. Hamilton, R. Winkler, and D. Culcer, Spin-orbit interactions in inversion-asymmetric two-dimensional hole systems: A variational analysis, Phys. Rev. B **95,** 075305 (2017).

[65] S. Bosco, M. Benito, C. Adelsberger, and D. Loss, Squeezed hole spin qubits in Ge quantum dots with ultrafast gates at low power, Phys. Rev. B **104,** 115425 (2021).

[66] C. Adelsberger, M. Benito, S. Bosco, J. Klinovaja, and D. Loss, Hole-spin qubits in Ge nanowire quantum dots: Interplay of orbital magnetic field, strain, and growth direction, Phys. Rev. B **105,** 075308 (2022).

[67] J.-W. Luo, A. N. Chantis, M. van Schilfgaarde, G. Bester, and A. Zunger, Discovery of a Novel Linear-in-*k* Spin Splitting for Holes in the 2D GaAs/AlAs System, Phys. Rev. Lett. **104,** 066405 (2010).

[68] A. A. High, A. T. Hammack, J. R. Leonard, S. Yang, L. V. Butov, T. Ostatnický, M. Vladimirova, A. V. Kavokin, T. C. H. Liew, K. L. Campman, and A. C. Gossard, Spin Currents in a Coherent Exciton Gas, Phys. Rev. Lett. **110,** 246403 (2013).

[69] M. V. Durnev, M. M. Glazov, and E. L. Ivchenko, Spin-orbit splitting of valence subbands in semiconductor nanostructures, Phys. Rev. B **89,** 075430 (2014).

[70] Y. Liu, J.-X. Xiong, Z. Wang, W.-L. Ma, S. Guan, J.-W. Luo, and S.-S. Li, Emergent linear Rashba spin-orbit coupling offers fast manipulation of hole-spin qubits in germanium, Phys. Rev. B **105,** 075313 (2022).

[71] M. Holthaus and B. Just, Generalized π pulses, Phys. Rev. A **49,** 1950 (1994).

[72] J. Roland and N. J. Cerf, Quantum search by local adiabatic evolution, Phys. Rev. A **65,** 042308 (2002).

[73] P. Richerme, C. Senko, J. Smith, A. Lee, S. Korenblit, and C. Monroe, Experimental performance of a quantum simulator: Optimizing adiabatic evolution and identifying many-body ground states, Phys. Rev. A **88,** 012334 (2013).

[74] D. Jirovec, P. M. Mutter, A. Hofmann, A. Crippa, M. Rychetsky, D. L. Craig, J. Kukucka, F. Martins, A. Ballabio, N. Ares, D. Chrastina, G. Isella, G. Burkard, and G. Katsaros, Dynamics of Hole Singlet-Triplet Qubits with Large *g*-Factor Differences, Phys. Rev. Lett. **128,** 126803 (2022).

[75] D. P. DiVincenzo, The physical implementation of quantum computation, Fortschritte der Phys. **48,** 771 (2000).

[76] L. H. Pedersen, N. M. Møller, and K. Mølmer, Fidelity of quantum operations, Phys. Lett. A **367,** 47 (2007).

[77] Y. Song, J. Li, Y.-J. Hai, Q. Guo, and X.-H. Deng, Optimizing quantum control pulses with complex constraints and few variables through autodifferentiation, Phys. Rev. A **105,** 012616 (2022).

[78] M. A. Nielsen and I. L. Chuang, *Quantum Computation and Quantum Information* (Cambridge University Press, New York, 2010), 10th ed.

[79] D. Stepanenko, M. Rudner, B. I. Halperin, and D. Loss, Singlet-triplet splitting in double quantum dots due to spin-orbit and hyperfine interactions, Phys. Rev. B **85,** 075416 (2012).

[80] P. M. Mutter and G. Burkard, Pauli spin blockade with site-dependent *g* tensors and spin-polarized leads, Phys. Rev. B **103,** 245412 (2021).

[81] A. Hofmann, D. Jirovec, M. Borovkov, I. Prieto, A. Ballabio, J. Frigerio, D. Chrastina, G. Isella, and G. Katsaros, Assessing the potential of Ge/SiGe quantum dots as hosts for singlet-triplet qubits (2019), ArXiv:1910.05841.

[82] P. M. Mutter and G. Burkard, All-electrical control of hole singlet-triplet spin qubits at low-leakage points, Phys. Rev. B **104,** 195421 (2021).